EUROPEAN ORGANIZATION FOR NUCLEAR RESEARCH

Proposal to the ISOLDE and Neutron Time-of-Flight Committee

Quantum colour centers in diamond studied by emission channeling with short-lived isotopes (EC-SLI) and radiotracer photoluminescence

13.05.2020

L.M.C. Pereira[1], U. Wahl[2], J.G. Correia[2], A.R.G. Costa[3], E. David Bosne[2], T.A.L. Lima[1], J. Moens[1], M.R. da Silva[4], M. Tunhuma[1], and A. Vantomme[1]

(The EC-SLI collaboration)

V. Amaral[4], P. Aprà[5], S. Ditalia Tchernij[5], J. Forneris[5], B. Green[6], K. Johnston[7], A. Lamelas[4], and P. Olivero[5]

[1] KU Leuven, Quantum Solid State Physics (QSP), 3001 Leuven, Belgium
[2] Centro de Ciências e Tecnologias Nucleares (C2TN), Instituto Superior Técnico, Universidade de Lisboa, 2695-066 Bobadela, Portugal
[3] CERN-TE, 1211 Geneva 23, Switzerland
[4] CICECO- Instituto de Materiais de Aveiro, Universidade de Aveiro, 3810-193 Aveiro, Portugal
[5] Physics Department and "NIS" Interdepartmental Centre, University of Torino, and Instituto Nazionale di Fisica Nucleare (INFN), 10125 Torino, Italy
[6] University of Warwick, Coventry CV4 7AL, UK
[7] CERN-EP, 1211 Geneva 23, Switzerland

Spokespersons: U. Wahl (uwahl@ctn.tecnico.ulisboa.pt)
L.M.C. Pereira (Lino.Pereira@kuleuven.be)
Local contact: J.G. Correia (Guilherme.Correia@cern.ch)

CERN-INTC-2020-037 / INTC-P-562
13/05/2020

Abstract

We propose studying the lattice locations of implanted radioactive isotopes of colour center elements in natural and synthetic diamond single crystals using emission channeling (EC), and to correlate this information with the optical properties of the centers as determined by radiotracer photoluminescence (PL). Our approach exploits the fact that EC has been the only experimental method capable of directly detecting and quantifying implanted impurities in diamond in the so-called "split-vacancy" configuration, which is supposed to be responsible for the remarkable optical properties of the centers. Moreover, in a new approach (on which so far nothing has been reported in the literature on diamond colour centers), we aim at investigating the influence of implantation temperature and of implantation under channeling conditions in order to critically reduce implantation-induced defects in diamond. The major effort will focus on studying the tin-vacancy (SnV^-) defect, currently one of the most-promising single photon emitters for quantum applications. However, other impurity colour centers that have been described in the literature and that are also envisaged to be addressed include Si, Ge, Pb, Mg, Ca, Sr, Ni, and also the noble gases He, Ne, Ar, Kr and Xe, although to a lesser extent than Sn.

Requested shifts: 20 shifts (split into ~8 runs over 2 years)

Motivation

The use of colour centers in diamond that are suitable as single photon emitters is currently at the forefront of efforts to establish crucial building blocks for a number of quantum technologies, in particular quantum information processing (which includes quantum cryptography and quantum computing) and quantum metrology (e.g. nano-sensors) [1-3]. One of the great challenges faced in that respect, is to controllably and efficiently introduce quantum colour centers, which consist of impurity atoms in very specific structural configurations, into diamond in such a way that they show the desired optical properties. For instance, for the lighter group-IV impurities Si, Ge, and Sn the so-called "split-vacancy configuration" (Fig. 1) is required [1-9]. However, it is not certain whether this configuration is also responsible for the optical activity of the heavy group-IV impurity Pb [10-11]. For less commonly studied colour centers, such as Mg [7, 12], Ca [12], Ni [1, 13] or the noble gases [14-15], in many cases very little theoretical work has been performed and the electronic structure of the optically active centers is still under debate. In some other cases, e.g. the so-called L1 or ST1 centers, even the chemical nature of these defects is still unclear, although they have been found to be very promising single photon emitters for quantum applications [12, 16].

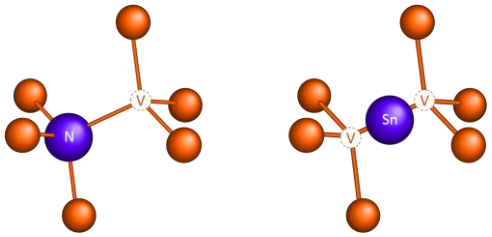

Fig. 1. The two major structures that are generally considered for impurity-vacancy complexes in diamond. With a carbon vacancy *V* next to it the nitrogen impurity N remains in a substitutional site (left), while for Sn the so-called split-vacancy configuration (right) has been proposed: the Sn atom moves from its substitutional site to a position midway between the two adjacent vacancies, which geometrically coincides with the so-called bond-center (BC) position in an undisturbed lattice.

Currently, ion implantation is the technique that is most widely used for creating colour centers [1-12, 14-16]. However, the efficiency of colour-center formation may be low or completely unknown, and the damage created by the implantation process adversely affects the luminescence linewidths and lifetimes of the centers. While the optical and electronic properties of the colour centers can be studied by the use of photoluminescence (PL) and magnetic resonance methods, there exist hardly any techniques that are capable of directly characterizing and quantifying their structural properties, i.e. atomic configurations and efficiency of structural formation. This is due to the simple fact that common structural characterization techniques such as ion beam analysis or X-ray related techniques completely fail at the low concentrations of colour centers required for quantum applications. This is illustrated by the example of Rutherford Backscattering Spectrometry/Channeling (RBS/C), which can be used to obtain information on the lattice sites of dopants in diamond only for implanted fluences well above 10^{14} cm^{-2} [17], while for quantum applications the required fluences are in the 10^{12} cm^{-2} range and below. Similarly, while X-ray Absorption Fine Structure (XAFS) spectroscopy has been used, e.g., to assess structural properties of Ni in diamond at the 10^{17} cm^{-2} level [13], this concentration is by many orders of magnitude above the interesting regime for quantum applications.

We propose to address the aspect of structural characterization of quantum colour centers in diamond by applying electron emission channeling (EC), a lattice location technique of unrivalled sensitivity (≈10^4 times more efficient than RBS/C) that is based on the use of radioactive isotopes [17] and well established at ISOLDE. The EC experiments shall be supplemented by radiotracer PL measurements, with the aim of establishing the chemical nature of PL lines of unknown or doubtful origin, but also for correlating the lattice location results with the optical properties (linewidth, intensity, lifetimes) of known luminescence lines.

Summary of previous results

As we have recently successfully demonstrated, the EC technique was able to assess the lattice sites of radioactive ^{121}Sn ($t_{1/2}$=27.06 h) implanted at a fluence of 2×10^{12} cm^{-2} into single-crystalline natural type IIa diamond [18]. Our data show that the split-vacancy configuration is formed immediately upon implantation with a surprisingly high efficiency of ≈40%. Upon thermal annealing at 920°C ≈30% of Sn is found in the ideal bond-center position (Fig. 2).

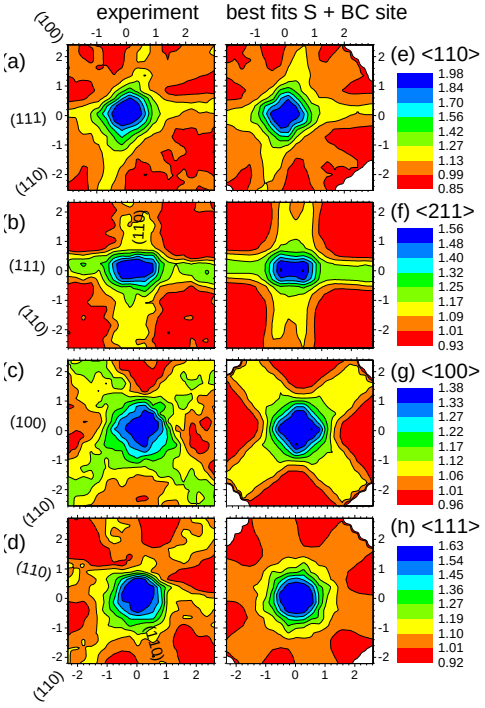

Fig. 2. (a)-(d): Experimental β^- emission channeling patterns from ^{121}Sn in diamond following 920°C annealing. The plots (e)-(h) are the corresponding best fits of theoretical patterns considering 70% on ideal substitutional and 30% on ideal bond-center sites. From Ref. [18].

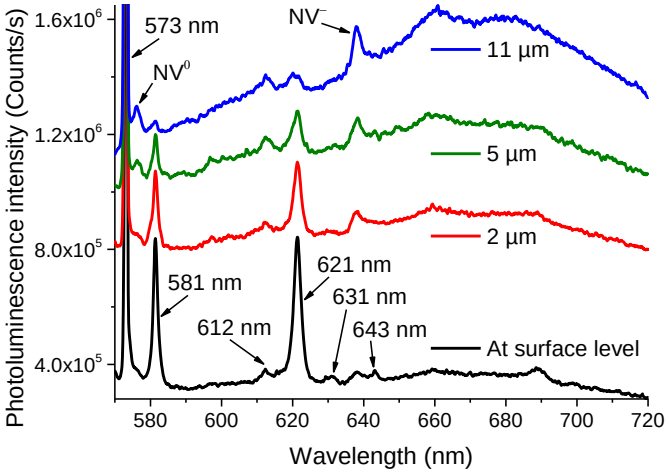

Fig. 3. Room temperature confocal PL spectra from diamond implanted with ^{121}Sn+^{121m}Sn ions after annealing at 920°C and following the decay of ^{121}Sn to ^{121}Sb, i.e. Sn*V* related lines result from long-lived ^{121m}Sn. The ZPL of SnV^- is clearly visible at 621 nm. The peak at 573 nm is the 1st order Raman line of diamond, while the prominent line at 581 nm could be due to the L1 center, a single photon emitting defect of unknown chemical origin [12, 16]. The bulk of the sample also shows lines due to NV^0 and NV^-. The spectra were recorded under 532 nm excitation with the focus at various depths (depth resolution ≈4 µm). From Ref. [18].

Around 50% of the mass 121 beam consisted of the long-lived isomer ^{121m}Sn (55 y), which made it possible to study the SnV^- luminescence properties following the EC measurements. Confocal PL revealed the characteristic SnV^- zero-phonon line (ZPL) at 621 nm, with an extraordinarily narrow RT ensemble linewidth (2.3 nm) of near-perfect Lorentzian shape (Fig. 3), just slightly larger than a recently found single center linewidth of 1.98 nm [9]). The PL spectra also revealed a sharp line at 581.4 nm (FWHM 1.5 nm), at the same wavelength as the L1 center (a bright quantum defect of unknown nature presenting a narrow ZPL at 581.7 nm [12, 16]). The depth distribution of the 581.4 nm line is correlated with the ZPL of SnV^-, hence a natural candidate for the chemical identity of this center would be ^{121}Sb, the decay product of ^{121}Sn.

Proposed experiments

The major focus of this proposal aims at the case of Sn*V*, on the one hand because SnV^- is currently among the hottest topics in diamond quantum colour centers [1-9], on the other hand because ^{121}Sn is a particularly suited probe for EC that can be reliably produced with high yields at ISOLDE from standard UC_x targets. From the difficult measurement conditions of the abovementioned diamond sample (an unusual surface cut 8° off <110>, requiring considerable efforts to orient it, nonetheless it was measured in the as-implanted and 920°C annealed state along 4 different crystallographic directions), we know that it will be possible to reduce the implanted ^{121}Sn+^{121m}Sn fluence by a factor of 4 and still obtain high-quality results for one annealing step. If it would be possible to tune the RILIS laser ionization to ^{121}Sn and thus suppress ^{121m}Sn in the beam, we should even be able to perform lattice location in the fluence range 2-3×10^{11} cm^{-2}. Complementarily, for higher fluences, lattice location experiments will be able to cover a whole sequence of annealing steps. Hence, in the course of 2021 we plan to accomplish a beam time with a number of ^{121}Sn emission channeling lattice location experiments. These should first aim at RT implantation of varying fluences in natural and CVD diamond, covering the range 5×10^{11}-5×10^{13} cm^{-2}, i.e. about almost 2 orders of magnitude of Sn concentration. This experimental approach should allow disentangling whether a difference in

the behaviour of Sn in natural and synthetic diamond exists, which seems plausible since synthetic diamond grown by the CVD technique may contain large amounts of H that could passivate the optical activity of Sn*V* centers, and whether such a possible effect is fluence-dependent. During the Sn beam time, also radiotracer PL on the ^{121}Sn→^{121}Sb decay should be performed at the ISOLDE PL lab. The main aim here is to identify the nature of the 581.4 nm line (possible L1) as well as some of the weaker lines indicated in Fig. 3, where doubts have been reported in the literature whether or not they are all Sn-related [5-9]. For instance, if the 581.4 nm line would be ^{121}Sn related, its intensity should decrease with time while it should increase for a ^{121}Sb related defect. In contrast, lines that are due to defects resulting from the implantation process should rather show constant intensity. Following the decay of ^{121}Sn, samples still contain the long-lived isomer ^{121m}Sn, which means that also the ^{121m}Sn*V*-related luminescence of the diamonds used already for emission channeling experiments can be studied, matching PL properties directly with the lattice location results that followed the last annealing step. In this case, gamma spectroscopy performed on the 37 keV decay line from ^{121m}Sn to ^{121}Sb will allow determining the amount of ^{121m}Sn dopants with % precision, thus providing reliable data for calculating optical activation yields that are independent from measurements of implantation currents.

As a next step, we aim at performing lattice location studies of ^{121}Sn where the implantation temperature is varied. To our surprise, we found no evidence in the literature of studies where quantum colour center elements were implanted in diamond above or below RT. This is despite the fact that it is well known that changing the implantation temperature has a huge effect on the accumulation of damage; in particular high-temperature implantation is much more efficient in preventing damage than subsequent annealing is in removing it [17]. In our EC-SLI on-line setup at ISOLDE, we can perform implantations in the temperature range from 50 K up to 900°C, which gives us a unique edge over many ion implantation labs that do not have such a wide temperature range available. At the moment it is difficult to predict whether heating or cooling the diamond sample during implantation will be beneficial with respect to Sn*V* formation and its optical properties. While heating will certainly reduce the number of defects that accumulate in the sample, which should lead to a narrowing of PL linewidths, it could also decrease the efficiency of Sn*V* formation, since the latter requires implanted Sn atoms to react not just with one but with two vacancies before these vacancies thermally anneal. The opposite may happen for implantation into cooled diamond. Another possibility of changing the defect production in a single crystal, which we also foresee to address, is implantation along major crystallographic axes, so-called channeling implantation. We know from our previous studies of GaN [17], that this can reduce damage creation by a factor of 5.

In addition to ^{121}Sn, exploratory studies will aim at other elements of particular interest as quantum colour centers in diamond. For instance, it is well established that the other group-IV elements Si and Ge also form colour centers whose optical properties can be explained by Si*V* or Ge*V* split-vacancy configurations [1-3]. However, direct structural evidence and formation efficiencies of these configurations upon ion implantation are lacking but could be determined from the amount of Si and Ge found on BC positions. In other cases, e.g. for Pb [10-11], Mg [7, 12], Ca [12], or Ni [1, 13], as well as for the noble gases He [14], Ne, Ar, Kr, and Xe [15], the exact structure of the optically active centers described in the literature is still under discussion, and EC lattice location can be expected to contribute solving this puzzle. Whenever possible, EC lattice location experiments should be combined with radiotracer PL (this is not feasible in all cases since e.g. He and Ne do not possess isotopes with suitable half-lives for radiotracer PL). Some of the colour center elements have isotopes for which routine production is well established at ISOLDE and we have used them already in EC experiments, e.g. ^{27}Mg, ^{45}Ca, ^{89}Sr, or ^{65}Ni. Others like ^{31}Al→^{31}Si (low yields) or ^{209}Pb (likely ^{209}Fr contamination) are more challenging and will require some discussions about optimization with the ISOLDE target group (however, we do at that point ***not*** ask for specific target development). We request short, exploratory beam times for as many isotopes as possible, aiming only at RT implantations in the 10^{12} cm^{-2} range or below. For channeling measurements of isotopes with half-lives shorter than ≈12 h our EC-SLI on-line setup at GHM will be used, for longer half-lives our off-line setups in building 508-R-008.

Summary of requested shifts:

Isotopes shown in **green** are for EC only; isotopes in **blue** are due to their half-lives also suitable for radiotracer PL; isotopes in **red** are precursors which are used for implantation and decay to the desired daughter probe isotopes. ***Please note that the number of shifts mentioned per isotope is tentative.*** As recently outlined in a letter to INTC, we request permission to be given some flexibility how to allocate the shifts in coordination with other users that would like to use the same targets. This also means we do not expect to be able to cover all listed isotopes within the next 2 years. However, with exception of ^{27}Mg, most of the requested isotopes can probably be produced either from UC-W or UC-plasma target-ion source combinations. For instance, for the noble gases a single UC-plasma run may be able to cover all requested isotopes. For isotopes produced from UC-W targets (the most common targets at ISOLDE), a bottleneck will be the availability of RILIS. Yields shown are taken from the ISOLDE development yield data base; beam currents during runs for implanting diamonds will be kept below 3×10^8 atoms/s.

isotope	half-life	yield (atoms/μC)	target - ion source	Shifts (8h)
^{121}Sn	**27.06 h**	1×10^8	UC_x-W - RILIS Sn	8
^{27}Mg	**9.5 min**	1×10^7	Ti-W - RILIS Mg	2.5
^{28}Mg	**21 h**	6×10^6	Ti-W or UC_x-W - RILIS Mg	0.25
^{45}K→**^{45}Ca**	17.3 min→**164 d**	1×10^7	UC_x-W	0.5
^{89}Rb→**^{89}Sr**	15.5 min→**50.5 d**	7×10^9	UC_x-W	0.25
^{65}Ni	**2.52 h**	7×10^7	UC_x-W - RILIS Ni	0.5
^{6}He	**807ms**	7×10^7	UC_x or BeO plasma	3.0
^{23}Ne	**37.2 s**	1.6×10^6	UC_x plasma	1.0
^{41}Ar	**109 min**	1.6×10^6	UC_x or TiO_2 plasma	0.5
^{87}Kr	**76.3 min**	2×10^8	UC_x or PbBi plasma	0.25
^{133}Xe	**5.2 d**	3×10^7	PbBi, ThC or UC_x plasma	0.25
^{135}Xe	**9.1 h**	1.5×10^8	ThC or UC_x plasma	0.25
^{31}Al→**^{31}Si**	644 ms→**157 min**	2.5×10^5	UC_x-W - RILIS Al	2
^{75}Ga→**^{75}Ge**	126 s→**82.8 min**	3×10^7	UC_x-W - RILIS Ga	0.5
^{209}Pb	**3.25 h**	no yield in data base	UC_x-Nb - RILIS Pb or LIST Pb	0.5
			Total shifts:	**20**

References:

[1] F. Lenzini, N. Gruhler, N. Walter, W.H.P. Pernice, *Diamond as a platform for integrated quantum photonics*, Advanced Quantum Technologies (2018) 1800061.

[2] D. Chen, N. Zheludev, W. B. Gao, *Building blocks for quantum network based on group-IV split-vacancy centers in diamond*, Advanced Quantum Technologies (2019) 1900069.

[3] C. Bradac, W. Gao, J. Forneris, M. E. Trusheim, I. Aharonovich, *Quantum nanophotonics with group IV defects in diamond*, Nature Comm. 10 (2019) 5625.

[4] S.D. Tchernij, T. Herzig, J. Forneris, J. Küpper, S. Pezzagna, P. Traina, E. Moreva, I.P. Degiovanni, G. Brida, N. Skukan, M. Genovese, M. Jakšić, J. Meijer, P. Olivero, *Single-photon-emitting optical centers in diamond fabricated upon Sn implantation*, ACS Photonics 4 (2017) 2580.

[5] T. Iwasaki, Y. Miyamoto, T. Taniguchi, P. Siyushev, M.H. Metsch, F. Jelezko, M. Hatano, *Tin-vacancy quantum emitters in diamond*, Phys. Rev. Lett. 119 (2017) 253601.

[6] A.E. Rugar, C. Dory, S. Sun, J. Vuckovic, *Characterization of optical and spin properties of single tin-vacancy centers in diamond nanopillars*, Phys. Rev. B 99 (2019) 205417.

[7] T. Lühmann, R. John, R. Wunderlich, J. Meijer, S. Pezzagna, *Coulomb-driven single defect engineering for scalable qubits and spin sensors in diamond*, Nature Comm. 10 (2019) 4956.

[8] M.E. Trusheim, B. Pingault, N.H. Wan, M. Gündoğan, L. De Santis, R. Debroux, D. Gangloff, C. Purser, K.C. Chen, M. Walsh, J.J. Rose, J.N. Becker, B. Lienhard, E. Bersin, I. Paradeisanos, G. Wang, D. Lyzwa, A.R.P. Montblanch, G. Malladi, H. Bakhru, A. Ferrari, I. A. Walmsley, M. Atatüre, D. Englund, *Transform-limited photons from a coherent tin-vacancy spin in diamond*, Phys. Rev. Lett. 124 (2020) 023602.

[9] J. Görlitz, D. Herrmann, G. Thiering, P. Fuchs, M. Gandil, T. Iwasaki, T. Taniguchi, M. Kieschnick, J. Meijer, M. Hatano, A. Gali, C. Becher, *Spectroscopic investigations of negatively charged tin-vacancy centres in diamond*, New J. Phys. 22 (2020) 013048.

[10] S.D. Tchernij, T. Lühmann, T. Herzig, J. Küpper, A. Damin, S. Santonocito, M. Signorile, P. Traina, E. Moreva, F. Celegato, S. Pezzagna, I.P. Degiovanni, P. Olivero, M. Jakšić, J. Meijer, P.M. Genovese, J. Forneris, *Single-photon emitters in lead-implanted single-crystal diamond*, ACS Photonics 5 (2018) 4864.

[11] M. E. Trusheim, N. H. Wan, K. C. Chen, C. J. Ciccarino, J. Flick, R. Sundararaman, G. Malladi, E. Bersin, M. Walsh, B. Lienhard, H. Bakhru, P. Narang, D. Englund, *Lead-related quantum emitters in diamond*, Phys. Rev. B 99 (2019) 075430.

[12] T. Lühmann, N. Raatz, R. John, M. Lesik, J. Rödiger, M. Portail, D. Wildanger, F. Kleißler, K. Nordlund, A. Zaitsev, J.F. Roch, A. Tallaire, J. Meijer, S. Pezzagna, *Screening and engineering of colour centres in diamond*, J. Phys. D: Appl. Phys. 51 (2018) 483002.

[13] E. Gheeraert, A. Kumar, E. Bustarret, L. Ranno, L. Magaud, Y. Joly, S. Pascarelli, M. Ruffoni, D.K. Avasthi, H. Kanda, *Investigation of nickel lattice sites in diamond: Density functional theory and x-ray absorption near-edge structure experiments*, Phys. Rev. B 86 (2012) 054116.

[14] J. Forneris, A. Tengattini, S.D. Tchernij, F. Picollo, A. Battiato, P. Traina, I.P. Degiovanni, E. Moreva, G. Brida, V. Grilj, N. Skukan, M. Jakšić, M. Genovese, P. Olivero, *Creation and characterization of He-related color centers in diamond*, J. Luminescence 179 (2016) 59.

[15] R. Sandstrom, L. Ke, A. Martin, Z. Wang, M. Kianinia, B. Green, W.B. Gao, I. Aharonovich, *Optical properties of Xe color centers in diamond*, Optics Comm. 411 (2018) 182.

[16] R. John, J. Lehnert, M. Mensing, D. Spemann, S. Pezzagna, J. Meijer, *Bright optical centre in diamond with narrow, highly polarised and nearly phonon-free fluorescence at room temperature*, New J. Phys. 19, 053008 (2017).

[17] L.M.C. Pereira, A. Vantomme, U. Wahl, *Characterizing defects with ion beam analysis and channeling techniques*, chapter 11 in: Characterisation and Control of Defects in Semiconductors, edited by F. Tuomisto (The Institution of Engineering and Technology, Stevenage, UK, 2019), p 501-561.

[18] U. Wahl, J.G. Correia, R. Villarreal, E. Bourgeois, M. Gulka, M. Nesládek, A. Vantomme, L.M.C. Pereira, *Direct structural identification and quantification of the split-vacancy configuration for implanted Sn in diamond*, submitted to Phys. Rev. Lett.

Appendix

DESCRIPTION OF THE PROPOSED EXPERIMENT

The experimental setups comprise: the EC-SLI on-line setup at GHM and 3 off-line EC setups dedicated to emission channeling experiments, the SSP collection chamber at GLM, and the ISOLDE SSP Photoluminescence Spectrometer

Part of the Experimental Setups	Availability	Design and manufacturing
(1) Emission Channeling setups	☒ Existing	☒ To be used without any modification EC-SLI setup at b.170-GHM [1] and off-line EC setups at b.508-R-008.
(2) SSP Photoluminescence Spectrometer	☒ Existing	☒ To be used without any modification The SSP photoluminescence spectrometer is permanently assembled in b.508-R-001 (edms documentation in preparation)
	☐ New	☐ Standard equipment supplied by a manufacturer ☐ CERN/collaboration responsible for the design and/or manufacturing
(3) SSP collection chamber(s) at GLM	☒ Existing	☒ To be used without any modification There are two chambers available for general purpose collection of radioactive isotopes mounted at GLM. These are generally mentioned as the (old) SSP collection chamber [2] that is still foreseen to be used as backup of the (new) ISOLDE general purpose collection chamber [3] during its commissioning.
	☐ New	☐ Standard equipment supplied by a manufacturer ☐ CERN/collaboration responsible for the design and/or manufacturing
[insert lines if needed]		

[1] https://edms.cern.ch/document/1960302/1 (EC-SLI setup)
[2] https://edms.cern.ch/document/1693386/1 (old SSP collection chamber)
[3] https://edms.cern.ch/document/1726781/1 (new SSP collection chamber)

HAZARDS GENERATED BY THE EXPERIMENT

Additional hazards:

Hazards	*(1)* *Emission Channeling setups*	*(2)* *SSP Photoluminescence Spectrometer*	*(3)* *SSP collection chamber(s) at GLM*
Thermodynamic and fluidic			
Pressure			
Vacuum	EC-SLI: 10^{-6} mbar, 40 L off-line: 10^{-6} mbar, 5 L	10^{-6} mbar, 2 L	old: 10^{-6} mbar, 20 L new: 50L (estimated)
Temperature	50 K up to 1173 K under vacuum	4.5 K up to RT under vacuum	
Heat transfer			
Thermal properties of materials	EC-SLI: Molybdenum sealed button heater off-line: filament heater		
Cryogenic fluid	Closed Cycle refrigerator (He)	Closed Cycle refrigerator (He)	
Electrical and electromagnetic			
Electricity	230 V, 15A	230 V, 15A	230 V, 15A
Electricity: detector HT	HT < 120 V dc, I < 100 μA		
Magnetic field	[magnetic field] [T]		
Batteries	☒ LOCAL UPS (GHM and 508-r-008)		
Capacitors	☐		
Ionizing radiation			
Target material	several types of Diamond samples	several types of Diamond samples	several types of Diamond samples
Beam particle type (e, p, ions, etc)	Singly charged ions		Singly charged ions
Beam intensity	see shifts table, will be limited to < 3E8 atoms/s		see shifts table, will be limited to < 3E8 atoms/s
Beam energy	> 30 keV		> 30 keV
Cooling liquids	[liquid]		
Gases	[gas]		
Calibration sources:	☐		
Open source	☐		
Sealed source	☐ [ISO standard]		
Isotope			
Activity			
Use of activated material:			
Description	☐		
Dose rate on contact and in 10 cm distance	We have estimated maximum sample activities from the count rates (CR) that saturate the EC detectors (4000 cps at the EC-SLI and 250 cps at the off-line setups, geometrical efficiency of the EC detectors at 30 cm from the sample is ~8E-4, so this corresponds to 5.0 MBq and 0.31 MBq). Rows in yellow denote experiments done on-line at the EC-SLI setup, where experimentalists are never closer than 30 cm to the sample which is behind 2 mm INOX chamber walls. The equivalent gamma dose rates (DRE gamma) are calculated for 10 cm in air. Rows in grey consider samples to be measured off-line at b.508. We considered Dose Rate Equivalent for betas (DRE beta) when there is the possibility to perform off-line experiments for EC (yellow rows) or PL (blue text), consequently requiring a closer manipulation using tweezers. Note that a typical diamond sample implanted with 2E12 atoms/cm-2 in a 1 mm beam spot initially contains 1.6E10 radioactive probe atoms. Activities necessary for PL experiments will generally be lower than those for EC experiments.		

	geo eff= (solid angle)	7.96E-04	**on-line max. detector CR** **4000 cps**	**on-line max. activity** **5.03E+06 Bq**	**off-line max. detector CR** **250 cps**	**off-line max. activity** **3.14E+05 Bq**

isotope	half-life	no atoms	DRE beta Hp(0.07)	DRE gamma (H10)	LA (MBq)
121Sn	27.06 h	4.41E+10	0.2 mSv/h	0	20
27Mg	9.5 min	7.05E+11	-	67 µSv/h	*na*
28Mg	21h	3.43E+10	0.40 mSv/h	6.0 µSv/h	3
45K→45Ca	164 d	6.42E+12	0.10 mSv/h	0	200
89Rb→89Sr	50.53 d	1.98E+12	0.40 mSv/h	8.0 µSv/h	200
65Ni	2.52 h	6.58E+10	6.7 mSv/h	36 µSv/h	40
6He	807ms	5.85E+06	-	no gamma	*na*
23Ne	37.2 s	2.70E+08	-	10 µSv/h	*na*
41Ar	109 min	4.74E+10	7.1 mSv/h	84 µSv/h	50
87Kr	76.3 min	3.32E+10	5.4 mSv/h	50 µSv/h	70
133Xe	5.2 d	2.04E+11	0.26 mSv/h	0.4 µSv/h	2000
135Xe	9.1h	1.48E+10	0.52 mSv/h	1.0 µSv/h	300
31Al→31Si	157 min	6.83E+10	6.7 mSv/h	no gamma	*na*
75Ga→75Ge	82.8 min	3.60E+10	7.5 mSv/h	2.5 µSv/h	90
209Pb	3.25 h	8.49E+10	7.5 mSv/h	no gamma	200

•			
•			
Non-ionizing radiation			
Laser		HeCd (wavelength 325nm, power ~50mW)	
UV light			
Microwaves (300MHz-30 GHz)			
Radiofrequency (1-300MHz)			
Chemical			
Toxic	[chemical agent], [quantity]		
Harmful	[chemical agent], [quantity]		
CMR (carcinogens, mutagens and substances toxic to reproduction)	[chemical agent], [quantity]		
Corrosive	[chemical agent], [quantity]		
Irritant	[chemical agent], [quantity]		
Flammable	[chemical agent], [quantity]		
Oxidizing	[chemical agent], [quantity]		
Explosiveness	[chemical agent], [quantity]		
Asphyxiant	[chemical agent], [quantity]		
Dangerous for the environment	[chemical agent], [quantity]		
Mechanical			
Physical impact or mechanical energy	[location]		

(moving parts)			
Mechanical properties (Sharp, rough, slippery)	[location]		
Vibration	[location]		
Vehicles and Means of Transport	[location]		
Noise			
Frequency	[frequency],[Hz]		
Intensity			
Physical			
Confined spaces	[location]		
High workplaces	[location]		
Access to high workplaces	[location]		
Obstructions in passageways	[location]		
Manual handling	[location]		
Poor ergonomics	[location]		

0.1 Hazard identification

3.2 Average electrical power requirements (excluding fixed ISOLDE-installation mentioned above): *(make a rough estimate of the total power consumption of the additional equipment used in the experiment)*